

CFD Analysis of Combined Serial Two Shell Pass Shell and Tube Heat Exchanger with Continuous Helical Baffles

Binu Varghese

*Department of Mechanical Engineering
Mar Athanasius College of Engineering, Kothamangalam*

Dr. Benny Paul

*Department of Mechanical Engineering
Mar Athanasius College of Engineering, Kothamangalam*

Gokul G Nair

*Department of Mechanical Engineering
Mar Athanasius College of Engineering, Kothamangalam*

Nidhin A R

*Department of Mechanical Engineering
Mar Athanasius College of Engineering, Kothamangalam*

Swagath V Mohan

*Department of Mechanical Engineering
Mar Athanasius College of Engineering, Kothamangalam*

Abstract

In the present era where energy demands are growing everyday it has become very important to capture every available energy from the hot source and utilize it for the process with minimum wastage. With this view, the combined serial two shell pass shell and tube heat exchanger (CSTSP) concept had been put forward and simulated using Fluent. Though the novel model of the heat exchanger has a higher heat transfer rate than the conventionally used segmental baffle heat exchanger but it poses a limitation with a higher pressure drop. This paper analyses the CSTSP model by incorporating certain changes in the geometry to try out two test cases namely CSTSP-B & CSTSP-C. Numerical analysis is performed on these models and their performance is compared with the original model. This study aims to put forward more insight on the performance of the CSTSP model heat exchanger to help researchers in future to optimize the geometric model and obtain a balance between heat transfer and pressure drop.

Keywords- CSTSP, Heat Transfer, Pressure Drop, Numerical Analysis

I. INTRODUCTION

Shell and tube heat exchangers are widely employed in almost all the process industries related to thermal applications and so the need to capture every joule of energy from the working fluid becomes very important. Extensive research has already been carried out and is still progressing in this area with the prime objective to maximize the heat transfer as much as possible from the system. Therein comes the problem with the process that in the wake of maximizing the heat transfer the pressure drop increases somewhat exponentially which directly adds to the pumping power and operating cost of the setup. Typically a shell and tube heat exchanger portrays segmental baffles inside the shell to guide the flow and induce turbulence. However these type of segmental baffles suffer from several disadvantages which make them unsuitable with the growing energy demands. Researchers have focused their attention on helical baffles which have become a good alternative for the segmental baffles. Stehlik et.al [1] carried out experimental tests to compare the performance of a helical baffle heat exchanger with the segmental baffle heat exchanger and found that the important parameter in a helical baffle is its helix angle and it needs to be optimized to get a balance between the heat transfer and pressure drop. Research by Zhang [2] showed that for middle overlapped helical baffles with 40° inclination angles had the best performance in terms of heat transfer. Taher et al focused on the impacts of baffle spacing for the discontinuous overlapped helical baffles for the inclination angle of 40°. Sandeep K Patel [3] studied the effects of mass velocity on the heat transfer coefficient under variable baffle spacing and baffle types. J Balabhaskar Rao [4] carried experimental tests on shell and tube heat exchangers with different circular and elliptical tube geometry profiles and found out that the elliptical tube profiles with mirror cut baffles showed 25% less pressure drop. B Peng [5] studied shell and tube heat exchanger with continuous helical baffles and compared the results with conventionally used segmental baffles. He found out that for the same mass flow rate and heat transfer area the helical baffles showed 10% higher heat transfer coefficient than the segmental baffle type. Dilip S Patel [6] made a comparison of all the turbulence models used in the simulation of heat exchangers and found out that of all the available models in Fluent the k-ε model showed much better accuracy with the experimental results. Studies were also conducted to optimize the performance of the heat exchanger and both conventional techniques like the Genetic Algorithm, Particle Swarm Optimization (PSO), Artificial Bee Colony (ABC) and other novel methods like Gravitational Search Algorithm were developed. Dilip Kumar Mohanty [7] studied ways on optimizing the heat exchanger from an economic point of view. Though the continuous helical baffles

prove to be a good choice yet the difficulty lies in their manufacturing but studies by Stehlik et al state that the manufacturing is difficult but it is one time investment and higher heat transfer performance will pay off rich dividends.

Recently Wang et al [8] proposed the combined serial two shell pass shell and tube heat exchanger with continuous helical baffles (CSTSP). In this model a central sleeve tube divides the shell into outer and inner shell. Fluid first flows in the outer shell and gets guided along the continuous helical baffles. Then through a U return the fluid then enters the inner shell where the diameter or the cross sectional area is much less than the outer shell. This causes the velocity to increase and thus leads to an increase in the heat transfer coefficient. The analysis presents a 31.2% rise in the value of heat transfer coefficient. However this occurs at the cost of a 130.9% rise in pressure drop. Because this is a novel concept therefore not much research has been done to study the performance of this type of heat exchanger which projects a much better heat transfer value. In this paper the performance of the CSTSP model heat exchanger is compared under two different geometrical conditions, one with an increased inner shell diameter (CSTSP-B) and the second one with helical baffles in the inner shell (CSTSP-C).

II. PHYSICAL MODELS

The physical dimensions of the CSTSP model heat exchanger are taken from the original paper while the two test cases have added dimensions and are shown in Fig 1. The baffle and sleeve thickness are taken as 2 mm with 1steel as material. The inner shell diameter for the test case B is 106mm while the helical baffle is placed concentric to the inner shell with outer diameter as 100mm equal to the value in the original case.

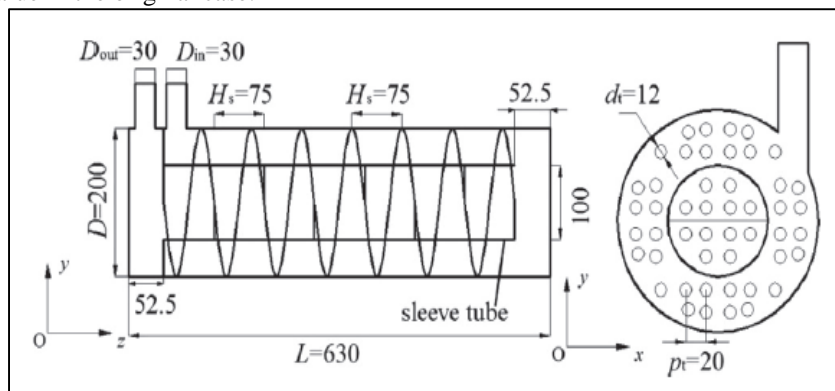


Fig. 1 (a): CSTSP- A (original model)

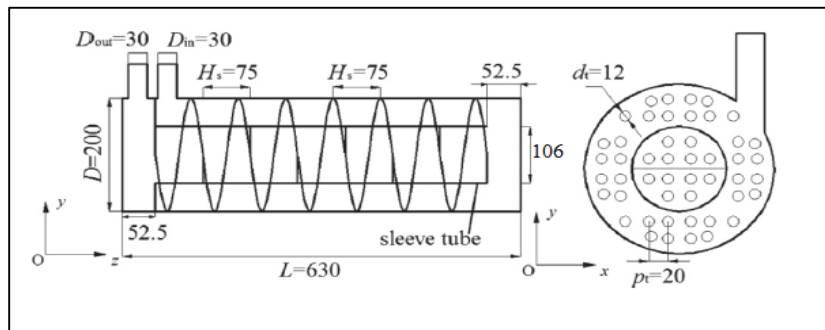


Fig. 1 (b): CSTSP- B (inner diameter 106mm)

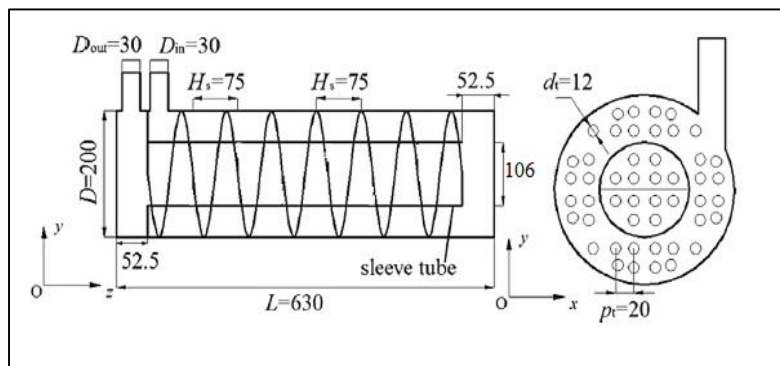


Fig. 1 (c): CSTSP- C (inner helical baffle)

Fig. 1: The physical model & test cases

Because of the large temperature difference between the inlet and outlet the material properties of water are dependent on temperature and the thermal properties of water are listed in table 1.

Table 1: Thermo-physical properties of water

Parameter	Expression (273<T<373)
$\rho(\text{kg/m}^3)$	$753.3+1.879*T-3.57*10^{-3}*T^2$
$c_p(\text{J/kg K})$	$10632.6-55.924*T+0.15968*T^2-1.4983.724*10^{-4}*T^3$
$\mu(\text{kg/m s})$	$0.11165-9.517*10^{-4}*T+2.724*10^{-6}*10^{-6}*T^2-2.6089*10^{-9}*T^3$
$\lambda(\text{W/m K})$	$-2.58673+2.399*10^{-2}*T-5.91953*10^{-5}*T^2+4.92088*10^{-8}*T^3$

A. Governing Equations

The turbulence model used is the realizable k-ε model with enhanced wall function. The k-ε model is well able to capture the physics of the flow under curvature, vortices or rotation. Here only the shell side analysis is done with the assumption that the flow and heat transfer are steady and turbulent, and the working fluid is incompressible. The governing equations are written below:

Continuity equation

$$\frac{\partial u_i}{\partial x_i} = 0 \tag{1}$$

Momentum Equation

$$\frac{\partial u_i u_j}{\partial x_i} = -\frac{1}{\rho} \frac{\partial p}{\partial x_i} + \frac{\partial}{\partial x_j} ((v + v_t) (\frac{\partial u_j}{\partial x_i} + \frac{\partial u_i}{\partial x_j})) \tag{2}$$

Energy equation

$$\frac{\partial u_i T}{\partial x_i} = \frac{\partial}{\partial x_i} ((\frac{v}{Pr} + \frac{v_t}{Pr_t}) \frac{\partial T}{\partial x_i}) \tag{3}$$

Turbulent kinetic energy k equation

$$\frac{\partial u_i k}{\partial x_i} = \frac{\partial}{\partial x_i} ((v + \frac{v_t}{\sigma_k}) \frac{\partial k}{\partial x_i}) + \mathcal{J} - \epsilon \tag{4}$$

Turbulent energy dissipation ε equation

$$\frac{\partial u_i \epsilon}{\partial x_i} = \frac{\partial}{\partial x_i} ((v + \frac{v_t}{\sigma_k}) \frac{\partial \epsilon}{\partial x_i}) + c_1 \mathcal{J} \epsilon - c_2 \frac{\epsilon^2}{k + \sqrt{v \epsilon}} \tag{5}$$

Where \mathcal{J} represents the generation of k and is given by

$$\mathcal{J} = -(u_i u_j)_{avg} \frac{\partial u_i}{\partial x_i} = v_t (\frac{\partial u_i}{\partial x_j} + \frac{\partial u_j}{\partial x_i}) \frac{\partial u_i}{\partial x_i} \tag{6}$$

$$v_t = c_\mu \frac{k^2}{\epsilon} \tag{7}$$

B. Boundary Conditions

The boundary conditions which are used are as follows:

- 1) Inlet fluid temperature:300K, mass flow rate: 4.2 kg/s
- 2) Outer wall: Adiabatic, non-slip boundary.
- 3) Tube wall: temperature:373K, non-slip boundary

The geometry of the model is developed in Solid works 2015 and imported to Ansys Fluent. The geometry is further subdivided into domains to create sweep able elements. Meshing is done in the fluent meshing module. Multizone method is used to mesh the geometry with prismatic elements. This reduces the cell count considerably. Inflation layer is grown on the tube walls and the outer wall with predetermined first cell height. A view of the meshed elements is shown in Fig 2.

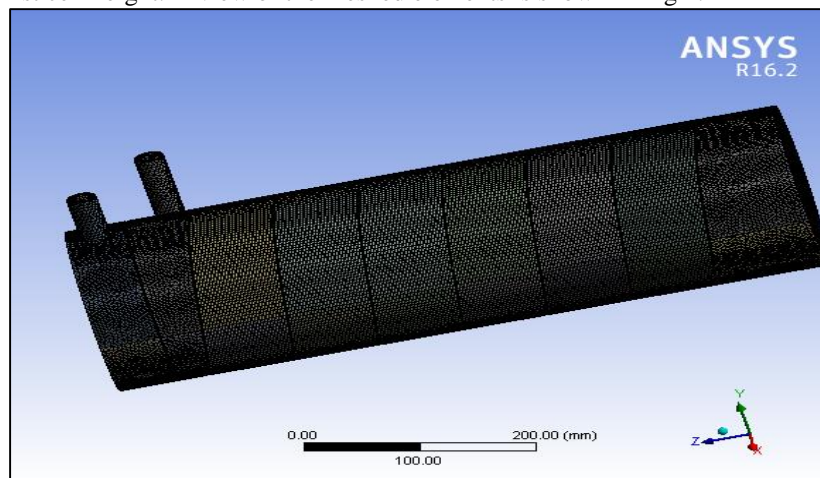


Fig. 2: Meshed model of CSTSP

C. Data Reduction

Heat transfer rate of shell – side fluid:

$$Q_m = c_p M (T_{out} - T_{in}) \tag{8}$$

Where T_{in} and T_{out} are the bulk temperatures of inlet and outlet. M is the mass flow rate. The shell-side heat transfer coefficient h is equal to:

$$h = Q_m / (\Delta T \cdot A_o) \tag{9}$$

$$\Delta T = \frac{\Delta T_{max} - \Delta T_{min}}{\ln(\Delta T_{max} - \Delta T_{min})} \tag{10}$$

$$\Delta T_{max} = T_w - T_{in} \tag{11}$$

$$\Delta T_{min} = T_w - T_{out} \tag{12}$$

$$A_o = N_t \cdot \pi \cdot d_t L \tag{13}$$

Where A_o is the heat transfer area; T_w is the temperature of tube walls.

D. Grid System and Validation

In order to get a grid independent mesh the simulation is tried with three test cases of meshes with body sizing so that mesh elements are 2586945,4042549,4886956 elements. The percent variation in results with last two mesh cases was less than 2% so the second mesh is taken for the simulation. In the paper by Wang [8] the cases are run for mass flow rates ranging from 1 to 5 kg/s. In this paper the same test is carried out and the maximum variation between the base paper results and the present work is 11.71% in pressure drop. Table II shows the results obtained in the present case for the original model and these results are compared with the paper values. Table III shows the results for one set of reading namely for mass flow rate of 4.2 kg/s.

Table 2: Simulation results for CSTSP – A

Mass flow rate, kg/s	Inlet temperature (K)	Outlet temperature (K)	Pressure drop ΔP , (Pa)
1.0	300	349.10	4779.57
2.0	300	348.26	24720.7
3.0	300	346.22	55079.4
4.2	300	345.24	113460

Table 3: Validation for the test case of Mass flow rate of 4.2 kg/s

	Outlet temp. (K)	Variation (%)	Pressure drop ΔP (Pa)	Variation (%)
Base Paper	355	2.74	120000	5.83
Present Work	345.24		113460	

III. RESULTS AND DISCUSSION

The analysis of temperature and pressure contour of the CSTSP-A model heat exchanger reveals many important facts which aid in understanding the behaviour of the CSTSP model. The model projects a higher heat transfer rate but also a higher pressure drop so it is important to find out the location of the maximum pressure drop region. Study of the temperature contour at the mid plane, Fig 3 reveals that color variation is maximum in the outer shell than in the inner shell and this is just a qualitative analysis. However by taking the section planes at inlet, near the far right end and in the outlet shows that about 76183Pa pressure drop occurs in the outer shell than in the inner shell. This is in agreement with the general idea that heat transfer occurs at the expense of drop in pressure.

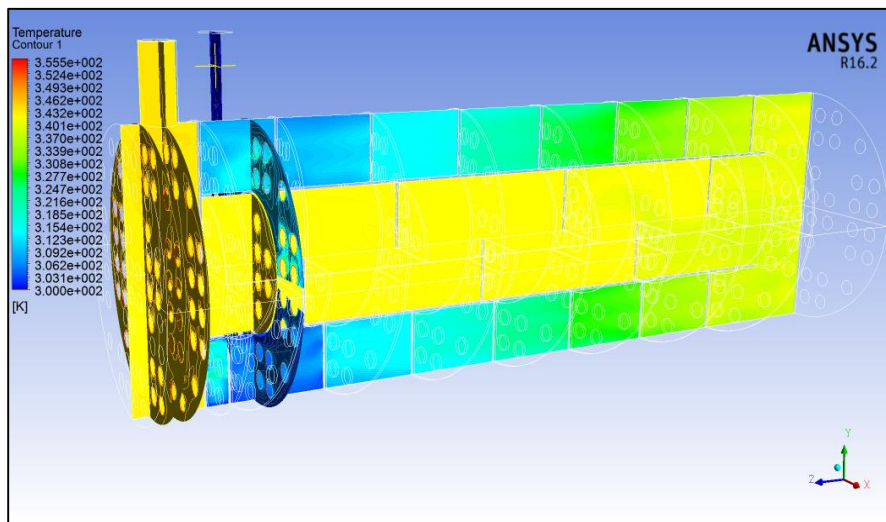


Fig. 3: Temperature contour at mid plane

Therefore the most obvious choice to lower the pressure drop or increase the outlet pressure will be to increase the inner shell diameter so that the inner area increases. But in order to capture the variations the increment in the diameter is very small that is from 100mm to 106mm. The table IV shows the results of the simulation which are carried out with this increased diameter.

Table 3: Results of simulation on CSTSP- B model

Mass flow rate, kg/s	Outlet pressure, (Pa)	Outlet temperature (K)	Change in outlet Pressure, $\Delta P(B-A)$ (Pa)	Change in outlet temperature $\Delta T (B-A)$, (K)
1.0	3241.28	354.54	+88.69	+5.44
2.0	12918.8	345.04	+370.9	-3.22
4.2	56869.6	338.82	+1368.6	-6.42

The results reveal that the increase in inner shell increase the outlet pressure or reduce the pressure drop and this is as expected. However the reduction in pressure drop is at the expense of the lower heat transfer as the outlet temperature decreases in the test case.

Fig 4 shows the temperature contour at the mid plane of the CSTSP-3 model. A qualitative look at the contour will not show any difference from the original model i.e. CSTSP-A. Table V presents the results of simulation for the third test case with helical baffles on the inner shell in place of the segmental baffles. The helical baffles are placed in order to investigate whether there is further increase in temperature or not.

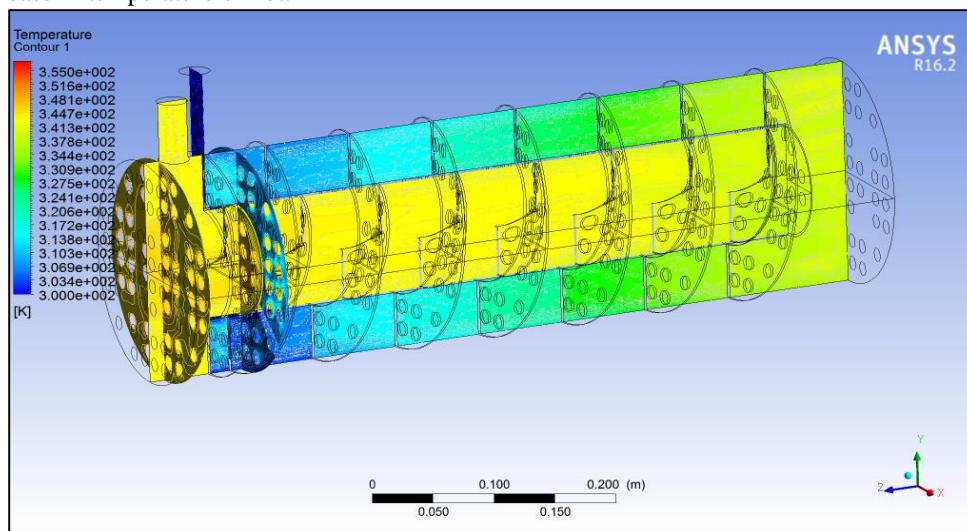


Fig. 4: Temperature contour at mid plane of CSTSP –C model

Table 4: Results of simulation on CSTSP- C model

Mass flow rate, kg/s	Outlet temperature (K)	Change in outlet temperature $\Delta T (C-A)$ (K)
1.0	351.72	+2.62
2.0	349.54	+1.28
4.2	346.23	+0.99

The results of this test case show that not much increase in the outlet temperature occurs with the addition of helical baffles on the inner shell as the temperature difference is less than 1°C in the case for 4.2 kg/s mass flow rate. Therefore looking from the view point of manufacturing difficulties and the initial cost this will not be beneficial to incorporate in the original model.

A. Comparison of Overall Performance

In order to gain a comparative insight among the performance of the three models graphs are plotted in terms of the mass flow rate, heat transfer rate and pressure drop. The number of tubes, tube layout, outer shell diameter are all maintained the same in the three models. Fig 5 shows the variation of heat transfer rate Q and pressure drop with respect to the mass flow rate for the three models. The graph reveals that the heat transfer rate increases almost linearly with the mass flow rate in all the three cases but the heat transfer rate of the CSTSP-B model is less than the other two models. This is because of the fact that the pressure drop in the B model is lower than the other two cases. The pressure drop increase with respect to the mass flow rate is almost exponential. However the drop increment in the CSTSP-C model is more than the other two cases for the same mass flow rate. Part of the reason is that because of the inner helical baffles the pressure in the outer shell increases rapidly and therefore the drop in pressure increases.

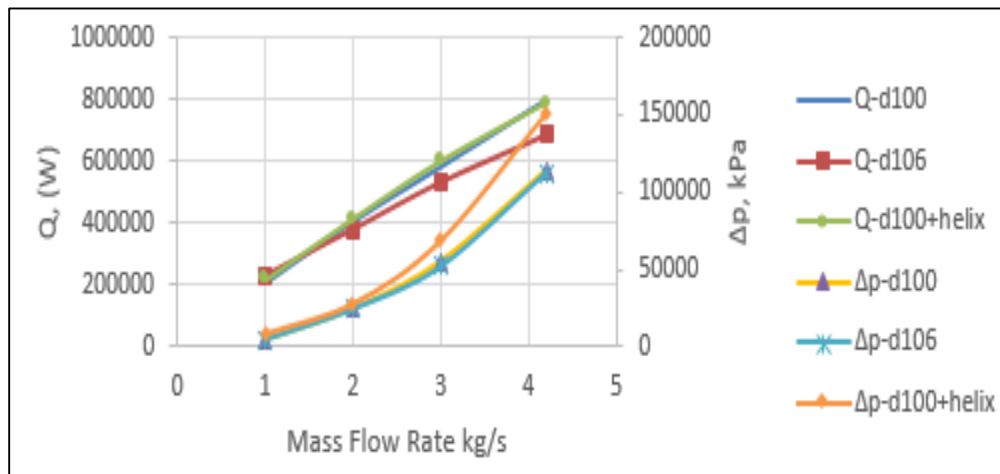


Fig. 5: Variation of Q and Δp versus M

The heat transfer rate and the pressure drop alone cannot be used to evaluate the performance of the heat exchanger and therefore parameters ' $Q/\Delta p$ ' are evaluated and plotted with respect to the mass flow rate. Fig 6 show the variation of these parameters with respect to M. The graphs reveal the fact that because the pressure drop is lower in CSTSP-B model therefore its performance is good as compared to the other two models. However the variation with original CSTSP-A is significantly more for a small increment in diameter with a little compromise with the heat transfer. Another point to note is that with increasing mass flow rate the performance graphs are almost similar showing that changes in the heat transfer rate and pressure drop are the same in all the three cases.

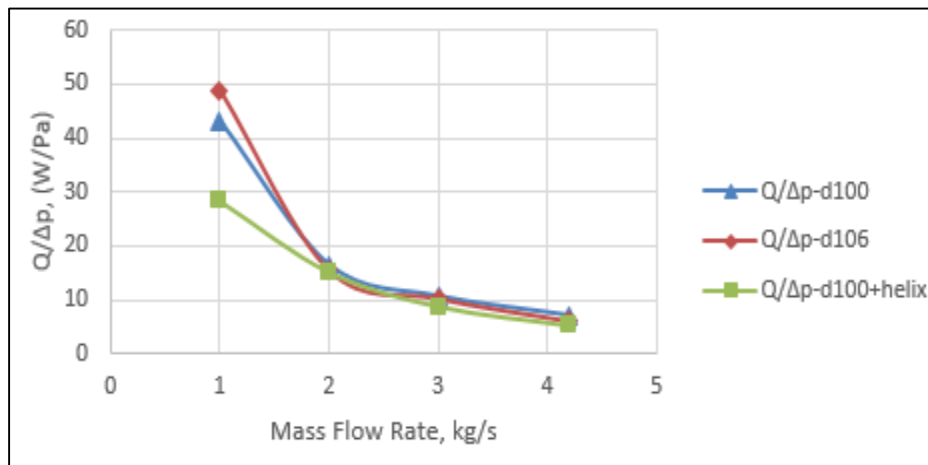


Fig. 6: Variation of $Q/\Delta p$ with Mass flow rate

IV. CONCLUSION

The performance of the combined serial two shell pass shell and tube heat exchanger with continuous helical baffles is evaluated by simulating the heat exchanger and three test cases are run one with increased inner diameter and the other with helical baffles on the inner shell. The results show that for lower mass flow rates increasing the inner shell diameter would be a good choice as it gives a lower pressure drop. However this effect is not dominant with increasing mass flow rate. This study is done in order to get an insight into the behaviour of the CSTSP model under different conditions and the study will help in developing an optimized configuration of this type of heat exchanger.

– Nomenclature

- A_o Heat transfer area (m^2)
- c_p Specific heat ($J/kg\ K$)
- c_i Coefficients in k- ϵ turbulence model
- D, D_s diameters of outer and inner shell (mm)
- h shell side average heat transfer coefficient ($W/m^2\ K$)
- I turbulence intensity
- k turbulent kinetic energy (m^2/s^2)
- M mass flow rate of working fluid (kg/s)

N_t	Number of heat exchange tube
Δp	Overall pressure drop (Pa)
Q	overall heat transfer rate (W)
T_w	Tube wall temperature
T_{in}, T_{out}	Inlet and outlet temperature (K)
ΔT	Logarithmic mean temperature difference (K)
T	fluid temperature (K)
–	Greek symbols
\mathcal{J}	Generalized diffusion coefficient
ε	dissipation rate of turbulence (m^2/s^3)
λ	Thermal conductivity (W/m K)
μ	dynamic viscosity (kg/m s)
μ_t	Turbulent dynamic viscosity (kg/ m s)
ν	kinematic viscosity (m^2/s)
ν_t	Turbulent kinematic viscosity (m^2/s)
ρ	density (kg/ m^3)
σ_k	Prandtl number of k
σ_ε	Prandtl number of ε

ABBREVIATION

CSTSP combined parallel two shell pass shell and tube heat exchanger

REFERENCES

- [1] Stehlik P, Nemicansky J. Comparison of correction factors for shell and tube heat exchangers with segmental or helical baffles. *Heat Transfer Eng* 1994; 15:55-65
- [2] Zhang JF, Li B, Huang WJ. Experimental performance comparison of shell side heat transfer for shell and tube heat exchanger with middle overlapped helical baffles and segmental baffles. *Chem Eng Sci* 2009; 64:1643-53
- [3] Sandeep K Patel. Shell and tube heat exchanger thermal design with optimization of mass flow rate and baffle spacing. *International Journal of advanced engineering research and studies* 2012 Vol II 130-135
- [4] J Balabhaskar Rao, V Ramachandra Raju. Numerical and Heat transfer analysis of shell and tube heat exchanger with circular and elliptical tubes. *International Journal of Mechanical and Material Engineering* 2016 Vol 11:6
- [5] B Peng, Wang QW. An experimental study of shell and tube heat exchanger with continuous helical baffles. *Journal of Heat Transfer – ASME* 2007; 129:1425-31
- [6] Dilip S Patel, Ravindrasinh R Parmar. CFD Analysis of Shell and tube heat exchangers- A review. *IRJET* 2015; Vol 2 Iss.9
- [7] Dilip Kumar Mohanty. Gravitational Search Algorithm for economic optimization design of a shell and tube heat exchanger. *Applied Thermal Engineering* 2016 Vol 6.133
- [8] Jian-Feng Yang, Min Zeng, Qiu-Wang Wang. Numerical Investigation on shell side performances of combined parallel and serial two shell pass shell and tube heat exchangers with continuous helical baffles. *Applied Thermal Eng.* 2014 Vol 11.029